J Fluoresc (2012) 22:1345–1356
DOI 10.1007/s10895-012-1074-9

ORIGINAL PAPER

Binding and Fluorescence Resonance Energy Transfer (FRET) of Ruthenium(II)-Bipyridine-Calixarene System with Proteins—Experimental and Docking Studies

P. Muthu Mareeswaran · D. Maheshwaran · E. Babu · S. Rajagopal

Received: 30 March 2012 / Accepted: 29 May 2012 / Published online: 15 June 2012

Abstract The investigation of the interaction of ruthenium (II)-bipyridine-*tert*-butylcalix[4]arene complexes (Rubc2 and Rubc3) with proteins (BSA and ovalbumin) using absorption, emission, excited state lifetime and circular dichroism techniques and by docking studies show that luminophore-receptor system bind strongly with proteins. An enhancement of absorption as well as emission intensity of Ru(II)-calixarene complexes in the presence of proteins, but the quenching of the emission intensity of proteins in the presence of Ru(II)-calixarene complexes are the interesting observations. The enhancement of emission intensity of Ru (II)-calixarene complex, in the presence of proteins, is due to the fluorescence resonance energy transfer (FRET) from protein to Ru(II)-calixarene complex. Among the two Ru (II)-calixarene complexes synthesized Rubc3 has more efficient binding and energy transfer than Rubc2 and BSA, with a large cavity size, has the advantage for binding over ovalbumin. Docking studies reveal that the presence of *tert*-butylcalix[4]arene moiety in Ru(II)-calixarene complexes facilitates binding with proteins. After the binding of Rubc2 and Rubc3 with proteins, the nearby fluorophores present in proteins are in optimal distance from the ruthenium centre for efficient FRET process to occur.

Keywords Ruthenium(II)-bipyridine-calixarene complexes · BSA · Ovabumin · FRET · Docking studies

Electronic supplementary material The online version of this article (doi:10.1007/s10895-012-1074-9) contains supplementary material, which is available to authorized users.

P. M. Mareeswaran · D. Maheshwaran · E. Babu · S. Rajagopal (✉)
School of Chemistry, Madurai Kamaraj University, Madurai 625021, India
e-mail: rajagopalseenivasan@yahoo.com

Introduction

Most of the anti-cancer agents are metallo-drugs [1, 2] and the serum proteins play a role for the transport of metallo-drugs. The binding of these metallo-drugs with serum will affect the delivery, distribution and local concentration of the drug at the disease site [3]. Therefore the study of interaction of metallo-drugs with blood serum proteins receives importance [3]. Human serum albumin (HSA), the most abundant plasma protein in the humans, [4, 5] plays a variety of roles in our body like controlling blood pressure, metabolism, radical de-activation and transport including drugs [6, 7]. The interaction of HSA with drugs may lead to a change in the drug stability and toxicity during the chemotherapy [4]. Since bovine serum albumin (BSA) has the 80 % structural similarity with HSA, BSA has been used as model by many group of researchers [4-8]. Though BSA is a dietary protein, the most important function of BSA is transportation [8-12]. This heart shaped protein, BSA has three homologous domains I–III [13] and each domain is made up of two subdomains, A and B, having unique binding properties [14]. BSA has two tryptophan residues, Trp-134 in the first domain and Trp-212 in the second domain. Trp-212 is located within a hydrophobic binding pocket and Trp-134 is on the surface of the molecule [14]. Trp-134 is available for the interaction with the binding molecules such as drugs [15]. The emission property of Trp-134 and Trp-212 depends on the microenvironment of the protein.

Another protein that has been taken for the present study is ovalbumin which is the major content of avian egg white [16]. Ovalbumin is widely used in the food industry and is also present in many biological systems [17]. Ovalbumin has slightly elongated ellipsoid structure with effective spherical diameter of 5 nm [18]. The formation of amyloid type cross-β structure is also possible in ovalbumin which is confirmed by its interaction with thioflavin T [19]. Both

BSA and ovalbumin can be used as drug carriers due to their biocompatibility and low cost [20-23].

The major anticancer agents used in the cancer chemotherapy are platinum compounds like cisplatin, and its second-generation derivatives, carboplatin and oxaliplatin [1, 2, 24, 25]. But these platinum complexes show high toxicity and are inactive against some tumors [26-28]. Among the other metal complexes, ruthenium(II)/(III) complexes are efficient alternatives for platinum [29-32]. Several studies show that organometallic complexes containing ruthenium(II) have promising anticancer characteristics [29] and some are also in clinical trials [31, 32]. Ruthenium (II)-polypyridyl complexes are also useful for the cellular uptake studies due to their stability in aqueous solutions and luminescencent properties [33-35]. Protein mediated transport and generation of activated (excited) Ru(II) species within tumors leads to the generation of reactive oxygen species responsible for the cytotoxic effect in photodynamic therapy (PDT) [36-40]. Binding of these metal complexes with proteins can modulate the activity of proteins [41]. Dendrimer type ruthenium(II)-polypyridyl complexes have also been reported for their surface binding ability with proteins [42, 43]. Metal complexes having large surface area and multivalency are expected to be useful for protein binding studies [44]. Increasing the hydrophobicity of the ruthenium drugs also controls the release of drug and cellular uptake [45].

In the present study *para-tert*-butylcalix[4]arene moiety is attached to ruthenium(II)-polypyridyl complex to increase the hydrophobicity. There are several reports on the surface binding studies of calixarenes [46-49]. Cellular uptake studies of calixarene derivatives show that contrary to the behavior of cyclodextrin, the uptake of calixarene leads to little deformation of the cell structure [50, 51]. Because of these advantageous properties the binding of calixarene receptors with proteins received importance [52]. Ungaro *et. al*. [53] have reviewed the application of multivalent calixarene ligands on lectin binding and inhibition, DNA condensation and cell transfection. Neri *et. al.* [54] have developed a histone deacetylase (HDAC) surface binding agent and established the surface binding properties of calixarene derivatives. Because of these interesting luminescent and binding properties of ruthenium(II) complexes and calixarenes pertaining to the biological system we have investigated the interaction of ruthenium(II)-calixarene system with proteins and important findings reported.

Experimental

The metal complexes, Rubc2 and Rubc3 (structure shown in Chart 1), are synthesized using the literature procedure [55] and characterized using HR-MS technique (The details are given in the supplementary material, Figs. S1 and S2). The mass values are very close to the literature values [55]. The BSA procured from Ocimum Bioscience and ovalbumin from Sigma-Aldrich are used without further purification. The double distilled deionized water is used in the preparation of phosphate buffer and this buffer is used throughout the study. The UV-visible absorption spectral studies are carried out using Analytik Jena Specord S100 spectrophotometer. The emission spectrum is recorded using Jasco FP 6300 spectrofluorometer. The circular dishroism (CD) measurements are carried out using Jasco polarimeter J180 at 2 cycles, 50 mm path length, 1 nm band width and 1 s response.

Excited state lifetime measurements were made with laser flash photolysis technique using an Applied Photophysics SP-Quanta Ray GCR-2(10) Nd:YAG laser as the excitation source. The time dependence of the luminescence decay is observed using a Czerny-Turner monochromator with a stepper motor control and a Hamamatsu R-928 photomultiplier tube. The production of the excited state on exposure to light of wavelength 355 nm was measured by monitoring (pulsed xenon lamp of 250 W) absorbance change. Here the wave length is fixed at the λ_{max} of emission in steady state method and the decay is measured. The natural log of the decay values is plotted against time which gives decay rate constant k. The inverse gives lifetime, τ of the complex.

Determination of Binding Constants

The binding constant of Rubc2 and Rubc3 with proteins is determined from the emission spectral data using Scatchard and Hills equations.

Scatchard Equation [56]

For emission measurements the concentration of Rubc2 and Rubc3 is fixed at 1×10^{-5} M and of protein is varied from 1×10^{-6} M to 9×10^{-6} M. We have used Scatchard equation for finding the cooperativity of the binding of Rubc2 and Rubc3 with proteins. The Scatchard equation shown in Eq. (1) is used to calculate the binding constant, K_a.

$$\upsilon/C_F = nK_a - \upsilon K_a \quad (1)$$

In Eq. (1) υ—ratio of the concentration of bound ligand to total available binding sites, C_F—number of binding sites per protein molecule, n—binding stoichiometry. The analysis of the data using the plot υ/C_F vs. υ shows that the plot is non-linear indicating the cooperative binding [56].

Hills Equation [57]

Since the Scatchard plot is non-linear we have calculated the binding constant using Hills equation, Eq. (2).

$$\log[\theta/(1-\theta)] = n\ \log[\text{protein}] - \log\ K_d \quad (2)$$

Chart 1 Structure of the ruthenium(II)-bipyridyl-calixarene complexes used in this study

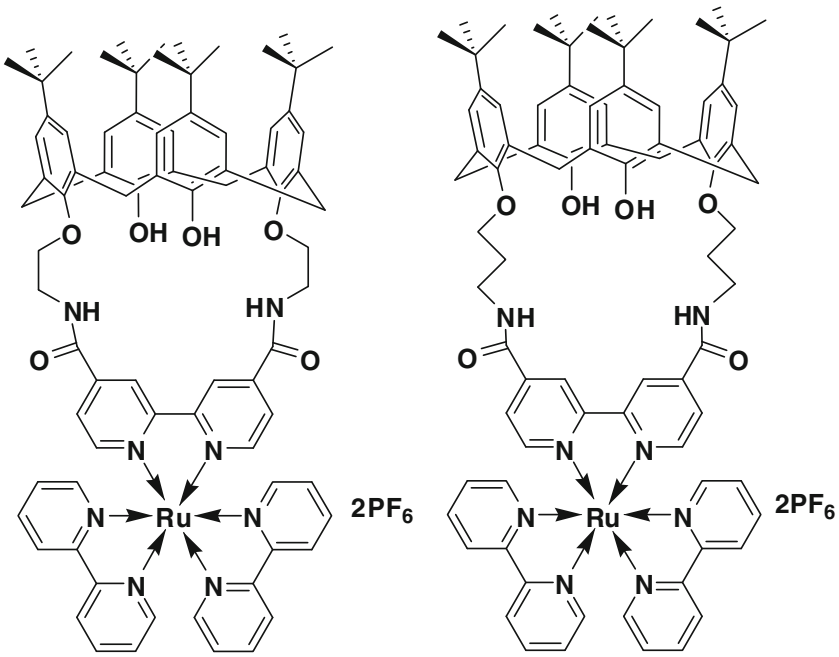

Here θ—number of binding sites (C_F in Scatchard equation), K_d—dissociation constant(the inverse of K_a), n—Hills coefficient of cooperativity which gives the nature of cooperativity. The value of n shows the nature of binding. $n>1$ positive cooperative binding, $n<1$ negative cooperative binding and $n=0$ non-cooperative binding. From the plot of log[θ/(1–θ)] vs log [protein] the value of n and K_d are calculated.

Estimation of Quenching Constant, k_q [58]

We have calculated the quenching constant (k_q) by using the Stern-Volmer equation Eq. (3),

$$F_0/F = 1 + k_q \tau [Q] \quad (3)$$

Here F_0 and F are the luminescence intensity of the luminophores in the absence and presence of quencher τ is the luminescence lifetime in the absence of quencher and [Q] is the concentration of quencher.

Measurement of Helicity of Proteins

For CD measurements the concentration of protein is fixed at 1×10^{-7} M and of Ru(II)-calixarene complex is varied from 1×10^{-5} to 3×10^{-5} M. The measurements were taken in Jasco polarimeter J180 at accumulation time 2 cycles, 50 mm path length, band width 1 nm, response 1 s. The helicity of the proteins is calculated by Eqs. (4) and (5) [59].

$$\text{Mean residual elipticity (MRE)} = \text{Observed CD}/\text{Cpnl} \times 10 \quad (4)$$

where, Cp—molar concentration of protein, n—number of amino acid residues, l—path length.

$$\alpha(\text{helix}\,\%) = (-\text{MRE} - 4000)/(33000 - 4000) \times 100 \quad (5)$$

In Eq. (5) 4000 is the MRE of the β–form and random coil conformation cross at the observed wavelength, and 33,000 is the MRE value of a pure α–helical at the observed wavelength.

Details of Docking Studies

The pdb (protein data bank) files of protein molecules have been downloaded from protein data bank (http://www.rcsb.org/pdb/home/home.do). Since there is no crystal structure available for BSA, the data from the crystal structure of HSA have been used for the study. Its file code is 1HA2 [60]. The pdb file used for the structure of ovalbumin is 1ugh [61]. The final model chosen is minimized using DISCOVER module of Insight II with 1,000 rounds of steepest descent and 1,000 rounds of conjugate minimization [62]. The cavity of the protein model has been picked by using Computed Atlas of Surface Topography of Proteins (CASTp) [63]. The docking towards the luminophores of proteins such as tryptophan and tyrosine has been done using GOLD [64]. For viewing the docked solutions and to generate pictures UCSF Chimera candidate version 1.5.3 is used [65].

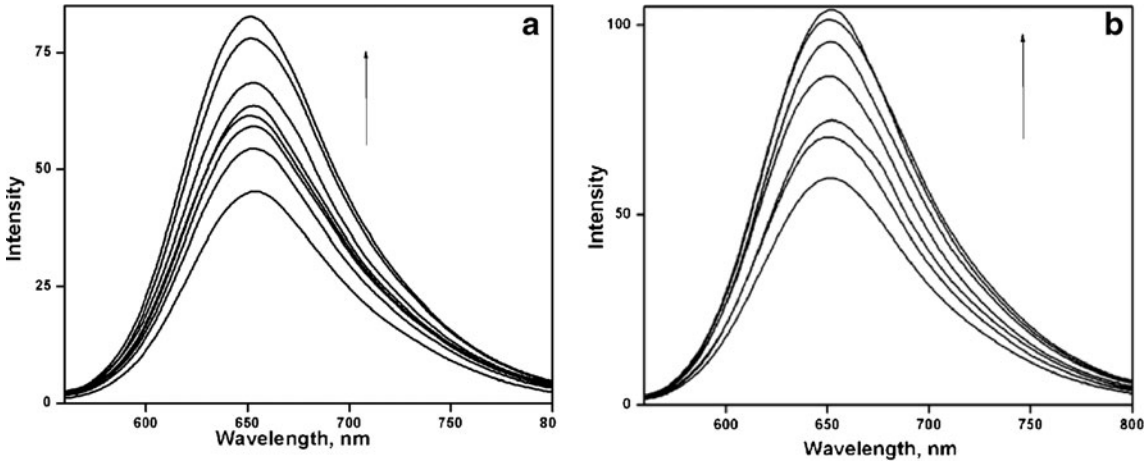

Fig. 1 Luminescence enhancement of (**a**) Rubc2 and (**b**) Rubc3 (1×10^{-5} M) on addition of increasing concentration of BSA (1×10^{-6}–9×10^{-6} M)

Results and Discussion

Steady State Absorption Spectral Study

The ruthenium(II)-bipyridine-calixarene complexes, Rubc2 and Rubc3 (Chart 1 gives structures) have been synthesized by literature methods [55]. All the spectral studies are carried out in phosphate buffer at pH 7.4. The concentration of Rubc2 and Rubc3 is fixed at 1×10^{-5} M and the concentration of BSA and ovalbumin is varied from 1×10^{-6} M to 9×10^{-6} M. The UV-visible spectra of Rubc2 and Rubc3 are recorded in the absence and in the presence of different concentration of proteins. There is a considerable change in the intensity of absorption corresponding to the ^{1}MLCT of Rubc2 and Rubc3. Due to the high molar extinction coefficient and experimental difficulties, higher concentration of protein has not been used i.e., the ratio of 1:10 is not maintained. Thus we have used lower concentration of proteins for the spectral study. With these concentrations we cannot apply Benesi-Hildebrand method for calculating binding constant. Therefore the binding constants are not calculated using absorption spectral technique. Absorption spectral technique is only used to show the enhancement of ^{1}MLCT absorption on the addition of proteins. The spectral changes are shown in supplementary material (Figs. S3 and S4). The substantial increase in the intensity of MLCT absorption on increasing the protein concentration shows strong binding of Rubc2 and Rubc3 with proteins. It is important to point out that the proteins have no absorption at this wavelength (450 nm).

Steady State Emission Spectral Study

The emission spectra of Rubc2 and Rubc3 show peaks at 653 nm and 658 nm respectively in the absence of proteins, upon using an excitation wavelength corresponding to their ^{1}MLCT absorption. When the protein is added to Rubc2 and Rubc3 we observe an increase in the emission intensity corresponding to emission of both complexes (Fig. 1). The enhancement in emission intensity of Rubc2 and Rubc3 in the presence of proteins indicates that there is binding of ruthenium(II) complex with proteins. The concentration of Rubc2 and Rubc3 is fixed at 1×10^{-5} M and the concentration of BSA and ovalbumin varied from 1×10^{-6} M to 9×10^{-6} M and the emission spectra of Rubc2 and Rubc3 are recorded in the presence of different concentrations of proteins. The emission spectral changes are shown in Fig. 1 and Fig. S5 (in supplementary material). Enhancement in the emission intensity at 650 nm is observed with an increase in [protein]. We have tried to use the Schatchard equation (Eq. (1)) to calculate the binding constant values of Rubc2 and Rubc3 with proteins. The Schatchard plots are shown in supplementary material (Figs. S6 and S7). The Scatchard plots in Figs. S6 and S7 show an upward curvature which indicates a negative-cooperative binding of the complexes with protein. So the binding constants cannot be calculated by these plots. Therefore the Hills equation (Eq. (2)) is used for the calculation of binding constant. The Hills plots are shown in in supplementary material (Figs. S8 and S9). The binding constant (K) and cooperativity (n) values calculated

Table 1 Binding constants (K_a) and quenching constants (k_q) and cooperativity (n) of the ruthenium(II)-bipyridine-calixarene complexes with proteins

Proteins	Rubc2 (M^{-1})			Rubc3 (M^{-1})		
	K_a, M^{-1}	n	k_q M^{-1} s^{-1}	K_a, M^{-1}	n	k_q M^{-1} s^{-1}
BSA	6.0×10^6	0.84	3.9×10^{13}	7.5×10^6	0.44	5.6×10^{13}
Ovalbumin	1.1×10^5	0.77	1.2×10^{12}	5.2×10^5	0.40	1.0×10^{12}

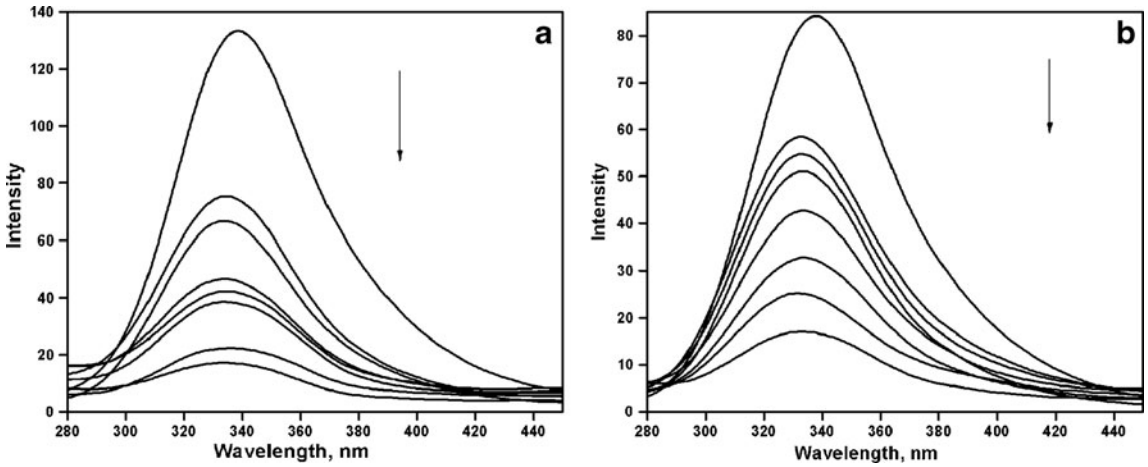

Fig. 2 Luminescence quenching of ovalbumin (1×10^{-5} M) in the presence of increasing concentration of (**a**) Rubc2 and (**b**) Rubc3 (1×10^{-5}–9×10^{-5} M)

from the Hills plot are collected in Table 1. From these binding constant values (10^5–10^6 M^{-1}) it is clear that the binding of Rubc2 and Rubc3 with proteins is very strong and comparable with the other Ru(II)-bipyridine complexes (10^5 M^{-1}) with cytochrome C [41] and Ru(II)-dendrimers (10^6 M^{-1}) with other proteins (chymotrypsin and lectin) [42, 43]. Ru(II)-calixarene complexes exhibit more efficient binding towards BSA compared to ovalbumin. Among the two Ru(II) complexes chosen Rubc3 exhibits more efficient binding than Rubc2.

The proteins, BSA and ovalbumin, contain fluorescent amino acids, such as phenyl alanine, tyrosine and tryptophan in their structure. The predominant fluorophore is tryptophan and its emission maximum, $\lambda_{max,}$ is around 348 nm. Hence, the emission intensity of protein is also monitored to understand more on the tryptophan environment. The concentration of the proteins is fixed at 1×10^{-5} M and the concentration of Rubc2 and Rubc3 is varied from 1×10^{-5}–9×10^{-5} M and the excitation wavelength is 280 nm. The results of the titration of Rubc2 and Rubc3 with BSA and ovalbumin are shown in Fig. 2 and Fig. S10 (in supplementary material) respectively. Since the molar extinction coefficient (∈) of the BSA and ovalbumin (43,000 mol^{-1} $cm^{-1}$and 58,800 mol^{-1} cm^{-1} respectively) is very high compared to that of Rubc2 and Rubc3 (2,351 mol^{-1} $cm^{-1}$and 1,721 mol^{-1} cm^{-1} respectively) at 280 nm the quantum of light absorbed by Ru(II) complexes at this wavelength is negligible. Therefore the observed luminescence quenching process is predominantly due to the energy transfer from the proteins to the Ru(II)-complexes, not due to the absorption of a part of light quanta by the Ru(II)-complexes at 280 nm. From this titration, quenching constants are calculated by using Stern-Volmer equation (Eq. (3)). The Stern-Volmer plots are shown in supplementary material (Figs. S11 and S12) and the quenching constant values are collected in Table 1. The average excited state lifetime of BSA and ovalbumin, 6.7 ns and 7.7 ns respectively have been used for the determination of k_q values [66, 67].

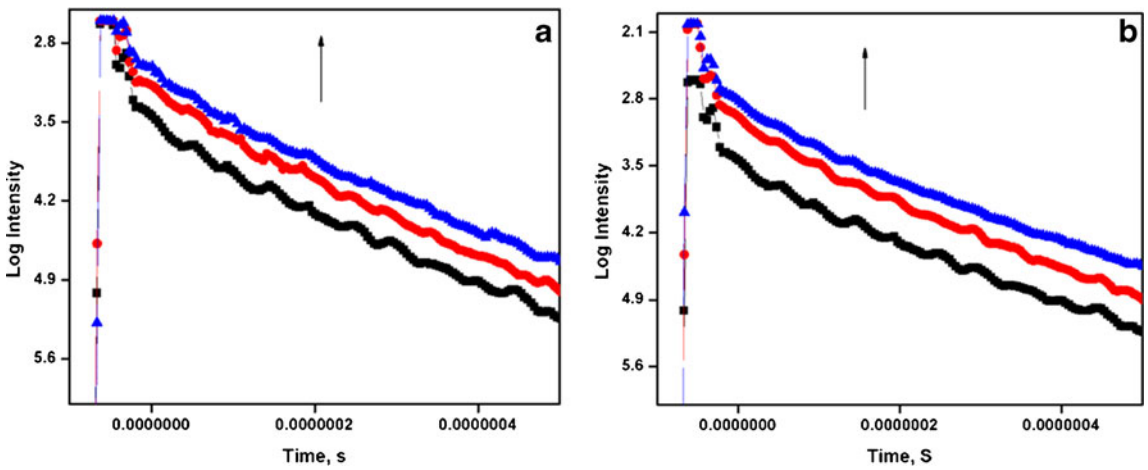

Fig. 3 Luminescence decays of (**a**) Rubc2 and (**b**) Rubc3 in the absence (*Black square*) and in the presence of BSA 1×10^{-5} M (*Red circle*) and 3×10^{-5} M (*Blue triangle*)

Table 2 Lifetime of the ruthenium(II)bipyridine-calixarene complexes in the presence of proteins at pH 7.4

	Rubc2 (ns)	Rubc3 (ns)
0	428	437
BSA		
1×10^{-6} M	432	449
3×10^{-6} M	460	496
Ovalbumin		
1×10^{-6} M	435	455
2×10^{-6} M	492	492

Since the quenching constants are in the range of 10^{12}–10^{13}, it is clear that the major contribution for the quenching process is from static quenching. There is a strong ground state complex formation, confirmed by the UV-visible absorption spectral titrations between the receptor and the protein and the binding constant values are in the range of 10^5–10^7 M^{-1}. The quenching constant value is comparatively higher for Rubc3 than Rubc2 for both proteins and is higher for BSA than ovalbumin for both complexes. It is interesting to note that similar results are observed with binding constants also. These large k_q values calculated in the present study show that the quenching process through energy transfer occurs on very fast time scale. Such high quenching constants for energy transfer have already been reported [68, 69] and can emphasize the occurrence of FRET process.

Excited State Lifetime Studies

The excited state lifetime of Rubc2 and Rubc3 is measured using emission mode of laser flash photolysis technique using 1×10^{-5} M Rubc2 and Rubc3. The details of measurement are given in the experimental section. The excited state lifetimes of Rubc2 and Rubc3, in the absence of proteins, are 428 ns and 437 ns respectively obtained by monitoring the emission at 650 nm and 653 nm. The lifetime decays are shown in Fig. 3 and Fig. S13 (in supplementary material). The excited state lifetime values are collected in Table 2.

The excited state lifetime of Rubc2 in the absence of proteins is 428 ns. The addition of 1×10^{-6} M of BSA and ovalbumin separately leads to a slight increase in the lifetime of Rubc2 to 432 and 435 ns respectively. On the other hand further increase in the protein concentration increases the lifetime of Rubc2 substantially to 460 and 492 ns respectively. Similar results are observed on the addition of BSA and ovalbumin with the other complex, Rubc3 as well. These results show that binding of Ru(II)-calixarene complexes with proteins results in the stabilization of these complexes in the excited state. It is important to recall that similar results are observed when luminescent ruthenium (II)-polypyridine complexes are added to DNA and surfactants [60-72].

Circular Dichroism Spectral Studies

To know about the structural changes of the proteins due to the binding of Rubc2 and Rubc3, the CD spectral studies have been carried out. The details of measurement are given under experimental section and the CD spectra are shown in Fig. 4 and Fig. S14 (in supplementary material). The CD spectral parameters are collected in Table 3.

The CD spectra of BSA in the absence and presence of Rubc2 and Rubc3 are shown in Fig. 4. When Rubc3 is added to BSA, considerable change is noted in the near UV–CD region 200–260 nm. This indicates that there is a significant alteration in the tertiary structure of proteins. From the changes in the CD spectrum, the α-helicity percentage can be calculated by Eq. 5. The native BSA has 66.8 % α-helicity. On the other hand addition of Rubc3 decreases the α-helicity substantially to 26.2 % and 14.9 % (Rubc3 1×10^{-7} M and 3×10^{-7} M, respectively). Addition of Rubc2 decreases the α-helicity to 53.8 % and 51.0 % (Rubc2 1×10^{-7} M and 3×10^{-7} M, respectively). In the case of native

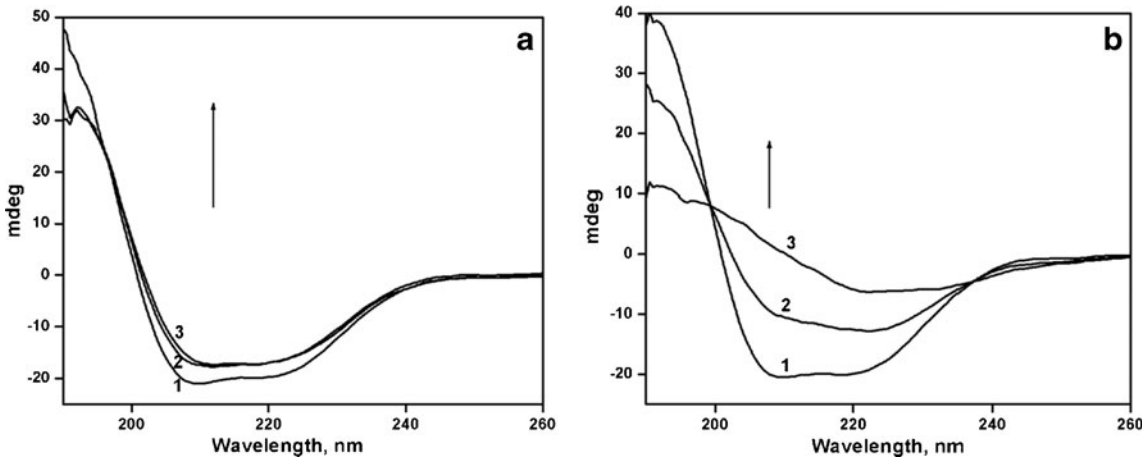

Fig. 4 CD Sepctra of BSA (3×10^{-7} M) in the absence (1) and in the presence of (**a**) Rubc2 at 1×10^{-7} M (2) and (**b**) Rubc3 at 3×10^{-7} M (3)

Table 3 CD parameters of BSA (3×10^{-7} M) and Ovalbumin (9.8×10^{-7} M) with interaction of complexes

Complex	BSA			Ovalbumin		
	λ_{max}	mdeg	α helicity	λ_{max}	mdeg	α helicity
Protein alone	209 222	−20.9125 −19.458	66.8 %	213	−24.8775	31.2 %
Rubc2 (1×10^{-7} M)	209 222	−17.1718 −16.774	53.8 %	213	−23.4622	29.0 %
Rubc2 (3×10^{-7} M)	209 222	−16.4049 −16.4396	51.0 %	217	−21.0881	24.6 %
Rubc3 (1×10^{-7} M)	209 222	−10.1867 −12.8055	26.2 %	220	−20.76768	24.0 %
Rubc3 (3×10^{-7} M)	209 222	−0.41378 −6.26035	14.9 %	218	−19.14558	21.1 %

ovalbumin, it has 31.2 % α-helicity. The addition of Rubc2 decreases the α-helicity of ovalbumin to 29.0 % and 24.6 % (Rubc2 1×10^{-7} M, 3×10^{-7} M respectively) and addition of Rubc3 decreases the α-helicity to 24.0 %, and 21.1 % (Rubc3 1×10^{-7} M, 3×10^{-7} M respectively). The decrease in the α-helicity of both BSA and ovalbumin is to a greater extent in the presence of Rubc3 compared to Rubc2. Compared to ovalbumin the change in α-helicity is higher for BSA toward both Rubc2 and Rubc3. These observations also support that the binding efficiency is higher for Rubc3 than Rubc2.

FRET from Proteins to Ru(II) Complexes

The FRET (fluorescence resonance energy transfer) finds extensive applications in life sciences to study the interaction of macromolecules especially with respective to their intra- and intermolecular interactions [73]. In clinical applications, FRET-based immunoassays are comparable with the radio immunoassays [74, 75]. As far as the present system is concerned the advantage is that the receptors, calixarenes, can bind with any molecule from small molecule like NO to very large molecule like proteins and even on the surface of a cell [76-78]. The importance of FRET in biochemistry is realized from its application that the efficiency of energy transfer can be used to evaluate the distance, r, between the probe and fluorophore residue in the protein [58]. According to the Forster's non-radiative energy transfer theory, [79] the rate of energy transfer depends on (i) the relative orientation of the donor (proteins) and the acceptor (Ru(II) complexes) dipoles, (ii) the extent of overlap of emission spectrum of the donor with absorption spectrum of the acceptor and (iii) the distance between the donor and the acceptor. The efficiency of energy transfer, E, is calculated using Eq. (6).

$$E = 1 - F/F_0 = R_0^6/\left(R_0^6 + r^6\right) \quad (6)$$

Here F and F_0 are the fluorescence intensities of proteins in the presence and absence of Rubc2 and Rubc3, r is the distance between the acceptor and the donor and R_0 is the critical distance when the transfer efficiency is 50 % and the value of R_0 is calculated by using Eqs. (7) and (8).

$$R_0^6 = 8.8\times10^{-25}\kappa^2\phi J N^{-4} \quad (7)$$

$$J = \Sigma F(\lambda)\varepsilon(\lambda)\lambda^4\Delta\lambda/\Sigma F(\lambda)\Delta\lambda \quad (8)$$

The term κ^2 is the relative orientation of space of the transition dipole of the donor and acceptor, ϕ is the quantum

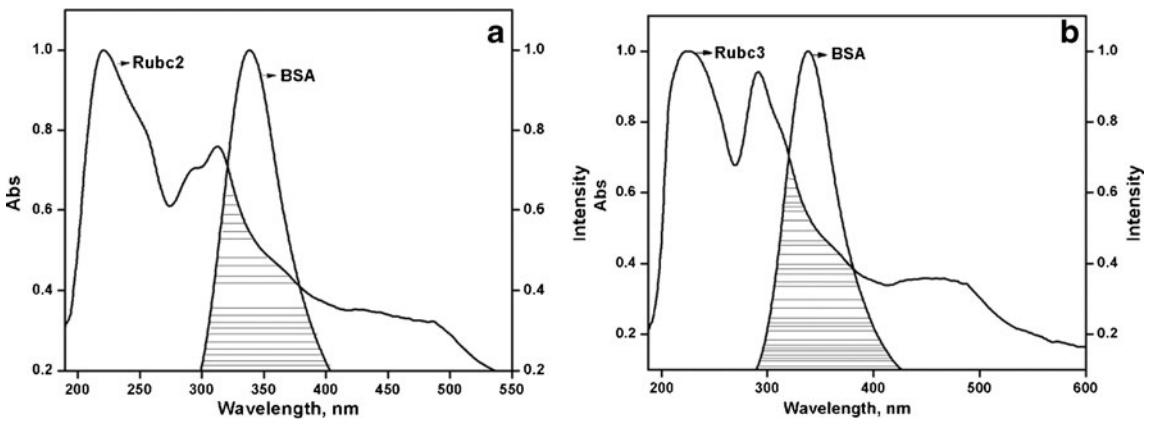

Fig. 5 Overlap integral of normalized emission spectrum of BSA with normalized absorption spectrum of (**a**) Rubc2 and (**b**) Rubc3

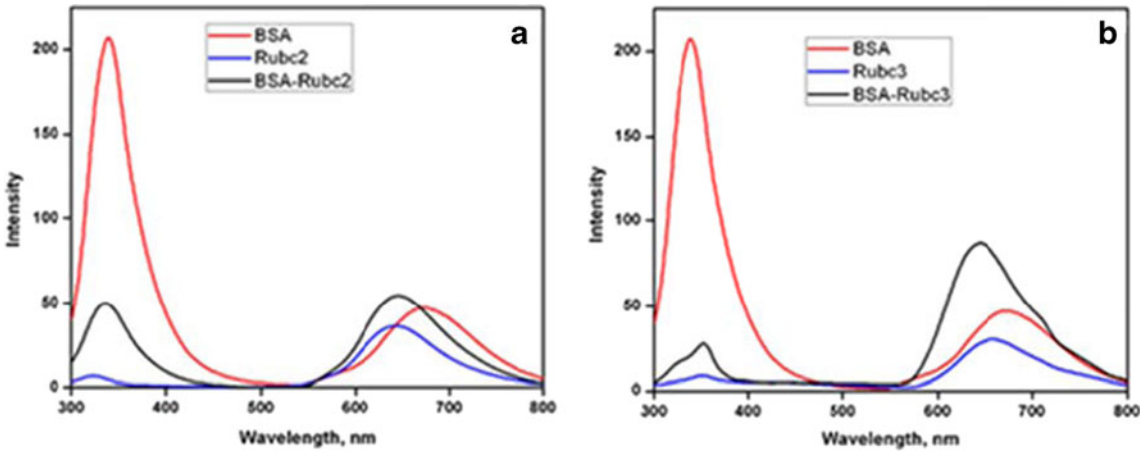

Fig. 6 Emission spectra of 1:1 mixture of (**a**) BSA and Rubc2 (**b**) BSA and Rubc3 excited at 285 nm

yield of the donor in the absence of acceptor, F(λ) is the fluorescence intensity of the fluorescent donor at the wavelength λ and is dimensionless, ε(λ) the molar absorption coefficient of the acceptor at λ and its unit is cm^{-1} M^{-1}.

Some interesting results are observed from the binding studies of Rubc2 and Rubc3 with proteins using emission spectral technique. When the emission spectra of Rubc2 and Rubc3 at the fixed concentration are recorded upon the addition of varying protein concentration, an enhancement of emission intensity is observed (Fig. 1 and Fig. S3 in supplementary material). On the other hand when we monitor the emission intensity at the fixed concentration of proteins upon varying the concentration of Rubc2 and Rubc3, quenching of emission intensity is observed (Fig. 2 and Fig. S10 in supplementary material). For the efficient energy transfer from the energy donor (proteins) to the acceptor (Rubc2 and Rubc3) the emission spectrum of the donor and absorption spectra of the acceptor must overlap. Figure 5 and Fig. S15 in supplementary material depict the overlap of the absorption spectrum of Rubc2 and Rubc3, respectively with the emission spectrum of BSA. These figures show that the overlap of absorption spectrum of Rubc2 and Rubc3 with the emission spectrum of BSA is efficient. Similar results are observed for complexes for the interaction of Rubc2 and Rubc3 with ovalbumin as well. To realize the presence of FRET we have taken a mixture of the protein and Rubc2/Rubc3 at the ratio 1:1, excited the solution at the excitation wavelength of protein (285 nm) and recorded the emission spectrum. The results are shown in Fig. 6 and Fig. S16 in supplementary material.

For this study the concentration of BSA and ovalbumin is fixed at 2×10^{-6} M and emission spectra are recorded from 300 to 800 nm using the excitation wavelength at 285 nm. The emission maxima, $\lambda_{max,}$ for BSA and ovalbumin are 339 nm and 331 nm respectively. The Rubc2 and Rubc3 are also excited separately at 285 nm and emission spectra recorded. The emission maxima, $\lambda_{max,}$ for Rubc2 and Rubc3 at the excitation wavelength 285 nm are 673 and 670 nm respectively. The 1:1 solution of BSA and Rubc2 is excited at 285 nm. The emission intensity at 339 nm of BSA is decreased but the λ_{max} of Rubc2 is blue shifted from 673 to 641 nm and emission intensity at this wavelength is enhanced. Similar results are obtained, when 1:1 ratio of BSA and Rubc3 is used. The values corresponding to emission spectral changes are collected in Table 4.

The enhancement of emission intensity is substantial for Rubc3 with blue shift in λ_{max}. Therefore the efficiency of energy transfer is more for Rubc3 than Rubc2. Similarly the enhancement of emission intensity and blue shift in λ_{max} is more substantial for BSA than ovalbumin which shows that the energy transfer is high for BSA. The values of energy transfer efficiency, r and R_0 values are collected in Table 5.

Table 4 Wavelength of emission maximum and intensity of 1:1 solution of proteins and Rubc2/Rubc3

	Complex alone		In the presence of			
			BSA		ovalbumin	
	λ_{max}	I	λ_{max} (nm)	I	λ_{max} (nm)	I
Protein alone			339	207.1	331	93.8
Rubc2	673	36.3	641	54.4	670	50.1
Rubc3	670	47.1	657	90.1	668	87.3

Table 5 FRET parameters of Rubc2 and Rubc3 with proteins

FRET couple	J	R_0 (nm)	r (nm)	Energy transfer efficiency
Rubc2-BSA	1.2×10^{-17}	7.7	4.8	72.1 %
Rubc3-BSA	1.9×10^{-17}	8.3	5.9	76.2 %
Rubc2-ovalbumin	1.2×10^{-17}	6.9	6.3	24.5 %
Rubc3-ovalbumin	1.7×10^{-17}	9.6	6.7	33.2 %

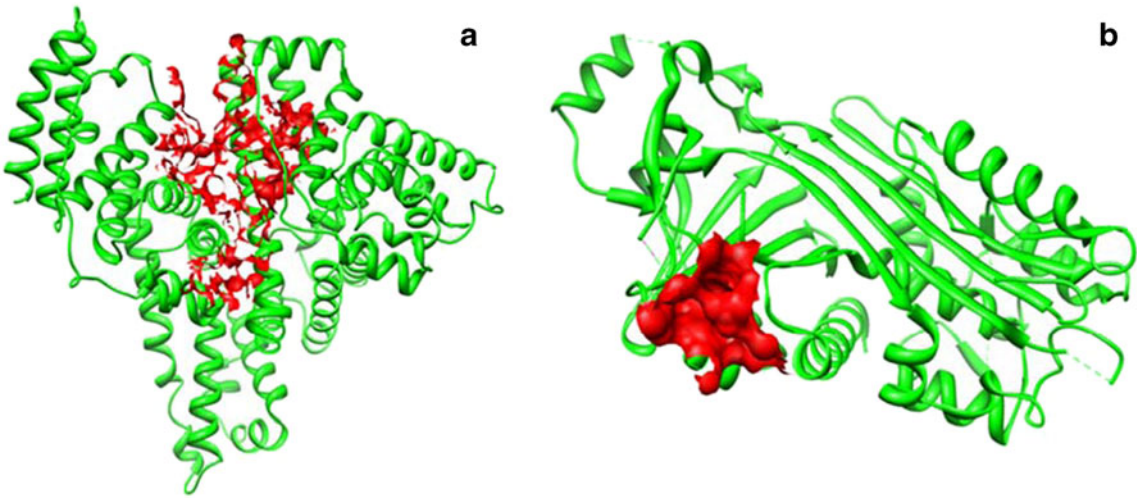

Fig. 7 Cavity of HSA (model to BSA) and ovalbumin using CASTp server

These calculations show that the energy transfer efficiency of Rubc3 is higher than Rubc2 and of BSA is higher than ovalbumin.

Docking Studies on the Binding of Rubc2 and Rubc3 with Proteins

From the above experimental results, it is clear that the complexes Rubc2 and Rubc3 bind efficiently with the two proteins. To gain more knowledge on the binding efficiency and the mode of binding we have carried out docking studies using GOLD software [70]. The details of the software and protein data bank (pdb) files are given in the experimental section. BSA has no crystal structure yet. Since HSA has 80 % similarity with the BSA we have downloaded HSA pdb file as model for BSA. The cavity of the proteins has been picked using an online tool, CASTp [69]. The cavities we have selected for HSA (model to BSA) and ovalbumin are shown in Fig. 7.

The hydrophobic surface area shown as red color in the cavity of the proteins is available for docking. Other cavities are also available but we have selected the biggest cavity for facile docking. The cavity volume for HSA (model to BSA) is 3587.5 $Å^3$ and of ovalbumin is 397.3 $Å^3$. Compared to the larger cavity available with HSA (model to BSA) for docking, ovalbumin has very small cavity which is also projecting outside of the protein. Since our study involves fluorescence as the technique and we are monitoring the fluorescence change experimentally, we identified the fluorophores (tryptophan, tyrosine and phenyl alanine) inside the cavity. Since the protein fluorescence is the collective fluorescence of tryptophan, tyrosine and phenyl alanine, we have chosen the TYR138 in HSA (model to BSA) and TYR125 in ovalbumin which are available inside the cavity

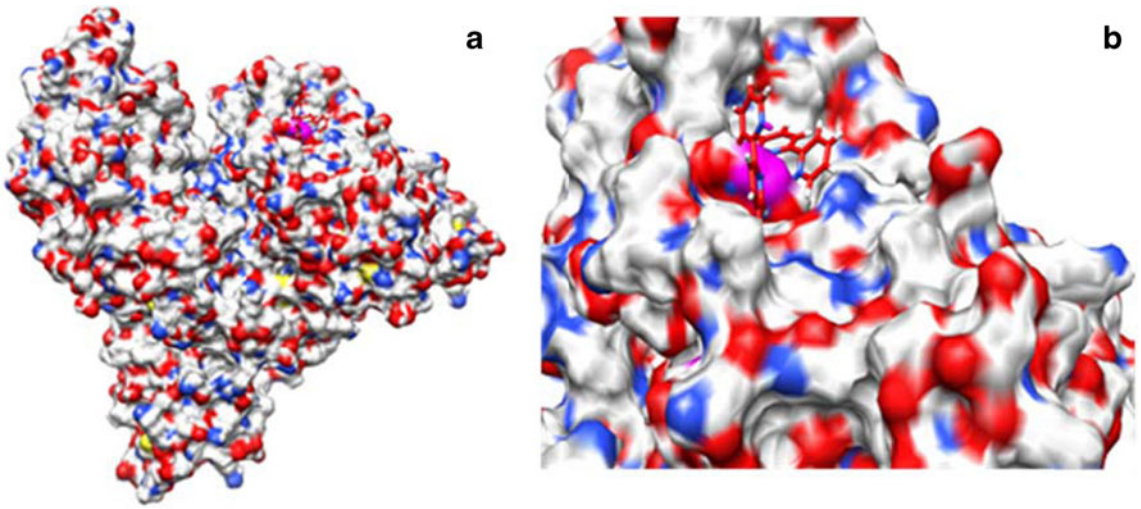

Fig. 8 Docking of Rubc3 with HSA (**a**) full view (**b**) closer view of the Ru(II) complex docked in protein

as the site of binding. The docked structures are shown in Fig. 8 and Fig. S17 in supplementary material.

Figure 8 and Fig. S17 in supplementary material illustrate the role of calixarene moiety in the binding with proteins. The calixarene moiety finely fits inside the hydrophobic cavity. The ruthenium(II)-bipyridine moiety is projecting outside of the proteins. Figure 8 shows that the calixarene moiety is totally buried in the hydrophobic cavity of the HSA (model to BSA). Therefore it is clear that the presence of calixarene moiety facilitates the efficiency of binding with proteins. The amino acid residues in proteins interact hydrophobically with *tert*-butyl group of calixarene moiety of two complexes as shown in supplementary material (Figs. S18 and S19) for HSA (model to BSA) and ovalbumin respectively.

The distance between the interacting *tert*-butyl group of calixarene and the amino acid side chains of proteins is given in Table S1 in supplementary material. Table S1 shows that the distance between the *tert*-butyl group of calixarene in both Rubc2 and Rubc3 and side chains of proteins ranges from 2.6 Å to 5.1 Å. The side chains of the amino acid groups in the proteins interacting with *tert*-butyl moiety are also hydrophobic in nature. These results exhibit that the hydrophobic nature of the *tert*-butylcalix[4] arene moiety plays important role in the binding of Rubc2 and Rubc3 with proteins.

Conclusion

This study provides an excellent luminophore-receptor system for efficient binding with proteins. The importance of calixarenes as receptors for the binding of proteins and cell surface is already realized. In the present study the attachment of *tert*-butylcalix[4]arene group enhances the hydrophobicity of the Ru(II) complex, which increases the binding efficiency. The steady state emission and docking studies show that the efficient binding results in the efficient FRET a useful tool in the biological systems. The CD spectral studies establish that the binding is more efficient for BSA than ovalbumin and for Rubc3 than Rubc2. The docking studies reveal that the *tert-butyl*-calix[4]arene group serves as anchoring group for the binding. As already indicated this system promises wide applications in biological and clinical systems because of extensive binding of calixarene with a large number of molecules and the possibility of efficient FRET process.

Acknowledgement We thank Prof. P. Ramamurthy, National Centre for Ultrafast Processes, University of Madras, Taramani, Chennai for his help in excited state lifetime studies. We thank Prof. S. Krishnasamy, School of Biotechnology, Madurai Kamaraj University for his help in the docking studies. We thank UGC-UPE for financial support. We thank Dr. M. Vairamani, IICT, Hyderabad for his help in taking HR-MS.

References

1. Timerbaev AR, Hartinger CG, Aleksenko SS, Keppler BK (2006) Interactions of antitumor metallodrugs with serum proteins: advances in characterization using modern analytical methodology. Chem Rev 106:2224–2248
2. Kratz F, Keppler BK (1993) Metal complexes in cancer chemotherapy. VCH, Weinheim
3. Fasanol M, Curry S, Terreno E, Galliano M, Fanali G, Narciso P, Notari S, Ascenzi P (2005) The extraordinary ligand binding properties of human serum albumin. IUBMB Life 57:787–796
4. Peters T Jr (1996) All about albumin. Academic, Orlando
5. Paul BK, Samanta A, Guchhait N (2010) Exploring hydrophobic subdomain IIA of the protein bovine serum albumin in the native, intermediate, unfolded, and refolded states by a small fluorescence molecular reporter. J Phys Chem B 114:6183–6196
6. Carter DC, Ho JX (1994) Structure of serum albumin. Adv Protein Chem 45:153–176
7. He XM, Carter CD (1992) Atomic structure and chemistry of human serum albumin. Nature 358:209–215
8. Mahanta S, Singh RB, Guchhait N (2009) Study of protein–probe interaction and protective action of surfactant sodium dodecyl sulphate in urea-denatured HSA using charge transfer fluorescence probe methyl ester of N, N-dimethylamino naphthyl acrylic acid. J Fluoresc 19:291–302
9. Singh RB, Mahanta S, Bagchi A, Guchhait N (2009) Interaction of human serum albumin with charge transfer probe ethyl ester of N, N-dimethylamino naphthyl acrylic acid: an extrinsic fluorescence probe for studying protein micro-environment. Photochem Photobiol Sci 8:101–110
10. Singh RB, Mahanta S, Guchhait N (2009) Study of proteinous and micellar icroenvironment using donor acceptor charge transfer fluorosensor N, N-dimethylaminonaphthyl-(acrylo)-nitrile. Spectrochim Acta Part A 72:1103–1111
11. Banerjee P, Pramanik S, Sarkar A, Bhattacharya SC (2009) Deciphering the fluorescence resonance energy transfer signature of 3-pyrazolyl 2-pyrazoline in transport proteinous environment. J Phys Chem B 113:11429–11436
12. Zhong D, Douhal A, Zewail AH (2000) Femtosecond studies of protein–ligand hydrophobic binding and dynamics: human serum albumin. Proc Natl Acad Sci USA 97:14056–14061
13. Bos OJM, Labro JFA, Ficher MJE, Witling J, Janssen LHM (1989) The molecular mechanism of the neutral-to-base transition of human serum albumin. J Biol Chem 264:953–959
14. Peters T (1985) Advances in protein chemistry. Academic, New York
15. Li D, Zhu M, Xu C, Ji B (2011) Characterization of the baicalein–bovine serum albumin complex without or with Cu^{2+} or Fe^{3+} by spectroscopic approaches. Euro J Med Chem 46:588–599
16. Sun Y, Hayakawa S (2002) Heat-induced gels of egg white/ovalbumins from five avian species: thermal aggregation, molecular forces involved, and rheological properties. J Agric Food Chem 50:1636–1642
17. Creamer LK, Jimenez-Flores R, Richardson T (1988) Genetic modification of food proteins. Trends Biotechnol 6:163–169
18. Stein PE, Leslie GW, Finch JT, McLauglin DJ, Carell RW (1990) Crystal structure of ovalbumin as a model for the reactive centre of serpins. Nature 347:99–102
19. Azakami H, Mukai A, Kato A (2005) Role of amyloid type cross â-structure in the formation of soluble aggregate and gel in heat-induced ovalbumin. J Agric Food Chem 53:1254–1257
20. Pearce FG, Mackintosh SH, Gerrard JA (2007) Formation of amyloid-like fibrils by ovalbumin and related proteins under conditions relevant to food processing. J Agric Food Chem 55:318–322

21. Chakraborty T, Chakraborty I, Moulik SP, Gosh S (2009) Physicochemical and conformational studies on BSA-surfactant interaction in aqueous medium. Langmuir 25:3062–3074
22. Kratz F (2008) Albumin as a drug carrier: design of prodrugs, drug conjugates and nanoparticles. J Contr Release 132:171–183
23. Welz MM, Ofner CM III (1992) Examination of self-crosslinked gelatin as a hydrogel for controlled release. J Pharm Sci 81:85–90
24. Wheate NJ, Walker S, Craig GE, Oun R (2010) The status of platinum anticancer drugs in the clinic and in clinical trials. Dalton Trans 39:8113–8127
25. Rosenberg B, Lippert B (1999) Cisplatin. Chemistry and biochemistry of a leading Anticancer Drug. Helvetica Chimica Acta, Zurich
26. Brabec V, Novakova O (2006) DNA binding mode of ruthenium complexes and relationship to tumor cell toxicity. Drug Resist Updat 9:111–122
27. Kelland LR, Sharp SY, O'Neill CF, Raynaud FI, Beale PJ, Judson IR (1999) Mini-review: discovery and development of platinum complexes designed to circumvent cisplatin resistance. J Inorg Biochem 77:111–115
28. Barnard PJ, Levina A, Lay PA (2005) Chromium(V) peptide complexes: synthesis and spectroscopic characterization. Inorg Chem 44:1044–1053
29. Hartinger CG, Zorbas-Seifried S, Jakupec MA, Kynast B, Zorbas H, Keppler BK (2006) From bench to bedside—preclinical and early clinical development of the anticancer agent indazolium trans-[tetrachlorobis(1H-indazole)ruthenate(III)] (KP1019 or FFC14A). J Inorg Biochem 100:891–904
30. Yan YK, Melchart M, Habtemariam A, Sadler PJ (2005) Organometallic chemistry, biology and medicine: ruthenium arene anticancer complexes. Chem Commun 4764–4776
31. Bruijnincx PCA, Sadler PJ (2008) New trends for metal complexes with anticancer activity. Curr Opin Chem Biol 12:197–206
32. Webb MI, Walsby CJ (2011) Control of ligand-exchange processes and the oxidation state of the antimetastatic Ru(III) complex NAMI-A by interactions with human serum albumin. Dalton Trans 40:1322–1331
33. Puckett CA, Barton JK (2010) Targeting a ruthenium complex to the nucleus with short peptides. Bioorg Med Chem 18:3564–3569
34. Puckett CA, Barton JK (2008) Mechanism of cellular uptake of a ruthenium polypyridyl complex. Biochemisty 47:11711–11716
35. Puckett CA, Barton JK (2007) Methods to explore cellular uptake of ruthenium complexes. J Am Chem Soc 129:46–47
36. Barragan F, Lopez-Senín P, Salassa L, Betanzos-Lara S, Habtemariam A, Moreno V, Sadler PJ, Marchan V (2011) Photocontrolled DNA binding of a receptor-targeted organometallic ruthenium(II) complex. J Am Chem Soc 133:14098–14108
37. Salassa L, Ruiu T, Garino C, Pizarro AM, Bardelli F, Gianolio D, Westendorf A, Bednarski PJ, Lamberti C, Gobetto R, Sadler PJ (2010) EXAFS, DFT, Light-induced nucleobase binding, and cytotoxicity of the photoactive complex *cis*-$[Ru(bpy)_2(CO)Cl]^+$. Organometallics 29:6703–6710
38. Clarke MJ (2002) Ruthenium metallopharmaceuticals. Coord Chem Rev 232:69–93
39. Bertozzi CR, Kiessling LL (2001) Chemical glycobiology. Science 291:2357–2364
40. Mann DA, Kanai M, Maly DJ, Kiessling LL (1998) Probing low affinity and multivalent interactions with surface Plasmon resonance: ligands for concanavalin A. J Am Chem Soc 120:10575–10582
41. Takashima H, Shinkai S, Hamachi I (1999) $Ru(bpy)_3$-based artificial receptors toward a protein surface: selective binding and efficient photoreduction of cytochrome c. Chem Commun 2345–2346
42. Ohkanda J, Satoh R, Kato N (2009) Protein surface recognition by dendritic ruthenium(II) tris(bipyridine) complexes. Chem Commun 6949–6951.
43. Kikkeri R, Garcia-Rubio I, Seeberger PH (2009) Ru(II)–carbohydrate dendrimers as photoinduced electron transfer lectin biosensors. Chem Commun 235–237.
44. Hamuro Y, Calama MC, Park HS, Hamilton AD (1997) A calixarene with four peptide loops: an antibody mimic for recognition of protein surface. Angew Chem Int Ed Engl 36:2680–2683
45. Scolaro C, Chaplin AB, Hartinger CG, Bergamo A, Cocchietto M, Keppler BK, Savab G, Dyson PJ (2007) Tuning the hydrophobicity of ruthenium(II)–arene (RAPTA) drugs to modify uptake, biomolecular interactions and efficacy. Dalton Trans 5065–5072.
46. Peczuh MW, Hamilton AD (2000) Peptide and protein recognition by designed molecules. Chem Rev 100:2479–2494
47. Zhou H, Wang D, Baldini L, Ennis E, Jain R, Carie A, Sebti SM, Hamilton AD (2006) Structure–activity studies on a library of potent calix[4]arene-based PDGF antagonists that inhibit PDGF-stimulated PDGFR tyrosine phosphorylation. Org Biomol Chem 2376–2386.
48. Park HS, Lin Q, Hamilton AD (2002) Modulation of protein–protein interactions by synthetic receptors: design of molecules that disrupt serine protease–proteinaceous inhibitor interaction. Proc Natl Acad Sci USA 99:5105–5109
49. Balskovich MA, Lin Q, Delarue FL, Sun J, Park HS, Coppola D, Hamilton AD (2000) Design of GFB-111, a platelet-derived growth factor binding molecule with antiangiogenic and anticancer activity against human tumors in mice. Nat Biotechnol 18:1065–1070
50. Grimmer S, van Deurs B, Sandvig K (2002) Membrane ruffling and macropinocytosis in A431 cells require cholesterol. J Cell Sci 115:2953–2962
51. Lalor R, Baillie-Johnson H, Redshaw C, Matthews SE, Mueller A (2008) Cellular uptake of a fluorescent calix[4]arene derivative. J Am Chem Soc 130:2892–2893
52. Perret F, Lazar AN, Coleman AW (2006) Biochemistry of the para-sulfonato-calix[n]arenes. Chem Commun 2425–2438.
53. Baldini L, Casnati A, Sansone F, Ungaro R (2007) Calixarene-based multivalent ligands. Chem Sov Rev 36:254–266
54. Chini MG, Terracciano S, Riccio R, Bifulco G, Ciao R, Gaeta C, Rroisi F, Neri P (2010) Conformationally locked calixarene-based histone deacetylase inhibitors. Org Lett 12:5382–5385
55. Szemes F, Hesek D, Chen Z, Dent SW, Drew MGB, Goulden AJ, Graydon AR, Grieve A, Mortimer RJ, Wear T, Weightman JS, Beer PD (1996) Synthesis and characterization of novel acyclic, macrocyclic, and calix[4]arene ruthenium(II) bipyridyl receptor molecules that recognize and sense anions. Inorg Chem 35:5868–5879
56. Lo KK, Tsang KH, Hui WK, Zhu N (2005) Synthesis, characterization, crystal structure, and electrochemical, photophysical, and protein-binding properties of luminescent rhenium(I) diimine indole complexes. Inorg Chem 44:6100–6110
57. Goto Y, Matsuno R, Konno T, Takai M, Ishihara K (2008) Polymer nanoparticles covered with phosphorylcholine groups and immobilized with antibody for high-affinity separation of proteins. Biomacromolecules 9:828–833
58. Lakowicz JR (2006) Principles of fluorescence spectroscopy, 3rd edn. Kluwer Academic Press, New York
59. Pan T, Xiao ZD, Huang PM (2009) Characterize the interaction between polyethylenimine and serum albumin using surface plasmon resonance and fluorescence method. J Lumin 129:741–745
60. Petitpas I, Bhattacharya AA, Twine S, East M, Curry S (2001) Crystal structure analysis of warfarin binding to human serum albumin. Anatomy of drug site I. J Biol Chem 276:22804–22809
61. Mol CD, Arvai AS, Sanderson RJ, Slupphaug G, Kavli B, Krokan HE, Mosbaugh DW, Tainer JA (1995) Crystal structure of human uracil-DNA glycosylase in complex with a protein inhibitor: protein mimicry of DNA. Cell 82:701–708
62. www.acceclrys.com

63. Dundas J, Ouyang Z, Tseng J, Binkowski A, Turpaz Y, Liang J (2006) CASTp: computed atlas of surface topography of proteins with structural and topographical mapping of functionally annotated residues. Nucl Acids Res 34:W116–W118
64. Verdonk ML, Cole JC, Hartshorn MJ, Murray CW, Taylor RD (2003) Improved protein-ligand docking using GOLD. Proteins 52:609–623
65. Pettersen EF, Goddard TD, Huang CC, Couch GS, Greenblatt DM, Meng EC, Ferrin TE (2004) UCSF Chimera—a visualization system for exploratory research and analysis. J Comput Chem 25:1605–1612
66. Ojha B, Das G (2010) The interaction of 5-(Alkoxy)naphthalen-1-amine with bovine serum albumin and its effect on the conformation of protein. J Phys Chem B 114:3979–3986
67. Kudryashova EV, Visser AJWG, van Hoek A, de Jongh HHJ (2007) Molecular details of ovalbumin-pectin complexes at the air/water interface: a spectroscopic study. Langmuir 23:7942–7950
68. Shih C, Museth AK, Abrahamsson M, Blaco-Rodriguez AM, Di Bilio AJ, Sudhamu J, Crane BR, Ronayne KL, Twine M, Vicek A Jr, Richards JH, Winkler JR, Gray HB (2008) Tryptophan-Accelerated electron flow through proteins. Science 320:1760–1762
69. Anula HM, Myshkin E, Guliaer A, Luman C, Danilov EO, Castellano FN, Bullerjahn GS, Rodgers MAJ (2006) Photo processes on self-associated cationic porphyrins and plastocyanin complexes 1. Ligation of plastocyanin tyrosine 83 onto metalloporphyrins and electron-transfer fluorescence quenching. J Phys Chem A 110:2545–2559
70. Tang Y, He F, Yu M, Wang S, Li Y, Zhu D (2006) Radical scavenging mediating reversible fluorescence quenching of an anionic conjugated polymer: highly sensitive probe for antioxidants. Chem Matter 18:3605–3610
71. Savariar EN, Gosh S, Gonzalez DC, Thayumanavan S (2008) Disassembly of noncovalent amphiphilic polymers with proteins and utility in pattern sensing. J Am Chem Soc 130:5416–5417
72. De Geest BG, Sanders NN, Sukhorukuv GB, Demmester J, De Semedt SS (2007) Release mechanisms for polyelectrolyte capsules. Chem Soc Rev 36:636–649
73. Cheng X, Bing T, Liu X, Shangguan D (2009) A label-free fluorescence sensor for probing the interaction of oligonucleotides with target molecules. Anal Chim Acta 633:97–102
74. Michalet X, Weiss S, Jager M (2006) Single-molecule fluorescence studies of protein folding and conformational dynamics. Chem Rev 106:1785–1813
75. Flehr R, Kienzler A, Bannwarth W, Kumke MU (2010) Photophysical characterization of a FRET system using tailor-made DNA oligonucleotide sequences. Bioconjucate Chem 21:2347–2354
76. Dalgarno SJ, Thallapally PK, Barbour LJ, Atwood JL (2007) Engineering void space in organic van der Waals crystals: calixarenes lead the way. Chem Soc Rev 36:236–245
77. Atwood JL, Barbour LJ, Jerga A (2004) A new type of material for the recovery of hydrogen from gas mixtures. Angrew Chem Int Ed 43:2948–2950
78. Hontama N, Inokuchi Y, Ebata T, Dedonder-Lardeux C, Jouvet C (2010) Structure of the calix[4]arene-(H2O) cluster: the world's smallest cup of water. J Phys Chem A 114:2967–2972
79. Forster T, Sinanoglu O (1996) Modern quantum chemistry, vol 3. Academic, New York